

INTRODUCTION: “Big Muley” is the largest rock collected on the Apollo missions. The bulk of the sample is a fragment-laden aluminous impact melt in which all plagioclase has been shocked to diaplectic glass. A chemically pristine but shocked and shock-melted anorthosite is a subordinate lithology. The shock-melted portion of the anorthosite was liquid, not diaplectic and intrudes the basalt (Fig. 1). Although the anorthosite has generally been referred to as a clast in the basalt, the contact of the non-melted anorthosite with the basalt is not in the thin sections and the relationships are obscure. Much of the rock is coated with a thin aluminous glass (Fig. 1). Warner et al.

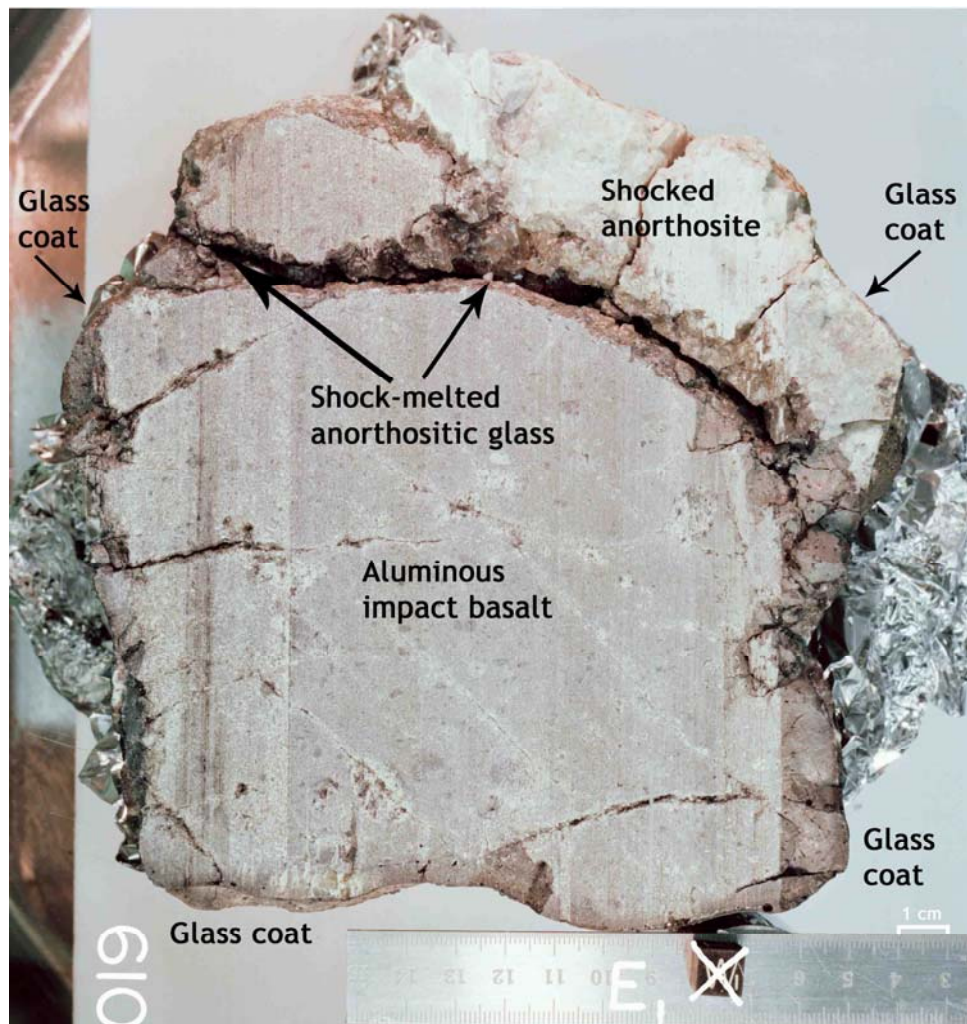


FIGURE 1. Sawn face of 61016 showing main lithologies and the fractures. S-78-33101

(1973) classify 61016 as a black-and-white rock: cataclastic anorthosite plus mesostasis-rich basalt.

61016 was collected from the east rim of Plum Crater and its orientation is known. Zap pits are absent from one side. This side was exposed on the lunar surface, indicating that a recent, and only recent, rotation of the sample occurred. Planar non-penetrative fractures are exposed on most surfaces.

PETROLOGY: 61016 consists of four lithologies: (i) basaltic impact melt, (ii) shocked anorthosite, (iii) shock-melted anorthosite glass and (iv) glass coat (Figs. 1 and 3). A proper appreciation of the published petrographic descriptions requires an understanding of the location of the thin sections studied; these are shown in Figure 2, except for thin sections made from 2 chips of white anorthosite.

Stoffler et al. (1975) give an extensive description of the petrography and petrogenesis of 61016 with emphasis on the basaltic impact melt (referred to as “spinel troctolitic matrix”) and the glass coat (“melt crust”). The paper provides microprobe analyses of minerals, metals, glasses, and xenoliths. Drake (1974), McGee et al. (1979) and Juan et al. (1974) describe thin sections which are composed of the impact melt and the anorthosite glass vein (from ,25).



FIGURE 2. Slab subdivisions. S-72-50692.

The basaltic impact melt (Fig. 3) consists of anhedral to subhedral olivine (43%), equant to lath-shaped anorthite transformed to diaplectic glass (42%), some tiny spinels, Fe-Ni metal (1.5%) and an opaque mesostasis (14%) consisting of ilmenite, submicroscopic

phases and glass (Stoffler et al., 1975). 16% of the basaltic lithology is xenolithic material. Olivine crystals are less than 200 μm and compositions range from Fo_{79-93} (Stoffler et al., 1975; Drake, 1974). Plagioclases are An_{92-98} (Stoffler et al., 1975). Fe-Ni-metal (Fig. 4) has 4.24-7.48% Ni and 0.24-0.47% Co (Misra and Taylor, 1975; Stoffler et al., 1975). The compositions of one metal-schreibersite pair indicates equilibrium at $\sim 650^\circ\text{C}$ (Misra and Taylor, 1975). Engelhardt (1979) notes that ilmenite occurs only in the mesostasis.

The chemically pristine shocked anorthosite is described by Steele and Smith (1973), Smith and Steele (1974), Stoffler et al. (1975), and Hansen et al. (1979a). It has a complex texture induced by shock metamorphism. Sub-rounded fine-grained, polycrystalline anorthite “bodies” (Stoffler et al., 1975) are embedded in a mass of spherulitically crystallized anorthite (Fig. 3). Some pyroxene aggregates are present. Plagioclases are An_{95-97} with low abundances of minor elements (Table 1) (Steele and Smith, 1973; Hansen et al., 1979a). Pyroxene blebs have two compositions, $\text{En}_{41}\text{Wo}_{44}$ and $\text{En}_{58}\text{Wo}_2$, lacking exsolution features on a 1 μm scale (Steele and Smith, 1973).

The shock-melted anorthosite glass is described by Juan et al. (1974), Drake (1974) and Dixon and Papike (1975) where it is referred to as the anorthosite. The confusion arises because the relevant thin sections have basaltic impact melt, shock-melted anorthosite, and a large diaplectic plagioclase which is probably a xenocryst in the basaltic melt rather than the anorthosite. The shock-melted anorthosite has the composition of nearly pure plagioclase (verified by our own partial analysis) (An_{96} ; Drake, 1974; Dixon and Papike, 1975). Some low-Ca pyroxene grains are present with compositions $\sim \text{En}_{64}$ (Dixon and Papike, 1975) as well as high-Ca pyroxene and Cr-spinel. Ishii et al. (1976) use pyroxene data from Dixon and Papike (1975) to find an equilibration temperature of 983°C .

The glass crust is described by Stoffler et al. (1975). It contains unshocked crystals and is connected to glass veins penetrating the rock. In places the glass coat has penetrated and annealed plagioclase in the basaltic impact melt. A temperature gradient of 600°C within about 2 mm is inferred (Stoffler et al., 1975).

CHEMISTRY: Abundant chemical data for 61016 lithologies have been published. In a few cases the lithology analyzed has been erroneously or not specifically reported; tables 2 and 3 list the references under the correct lithologies. In most cases the analyses are reported without specific comment.

The basaltic impact melt (Table 4) (61016 “dark”) is aluminous and siderophile-rich. Ganapathy et al. (1974) place it in their meteorite Group 1. REEs are 45 (light)-20 (heavy) times chondrites i.e., a KREEP pattern (Fig. 5). Although roughly similar to local soils (Laul and Schmitt, 1973), in detail it differs significantly e.g., higher magnesium, lower nitrogen. The impact melt is volatile-enriched but when that enrichment occurred is not defined: Krahenbuhl et al. (1973) note that both the impact melt and the anorthosite have similarly high Tl contents, suggesting post-formational enrichment. However, Cd and In are enriched in the impact melt as compared to the anorthosite (Krahenbuhl et al., 1973; Wasson et al., 1975) suggesting pre-formational

enrichment. While impact melt has even higher contents of the volatiles Cl and Br than does 66095 (Jovanovic and Reed, 1973; and others), it has much lower abundances of Zn, even lower than local soils.

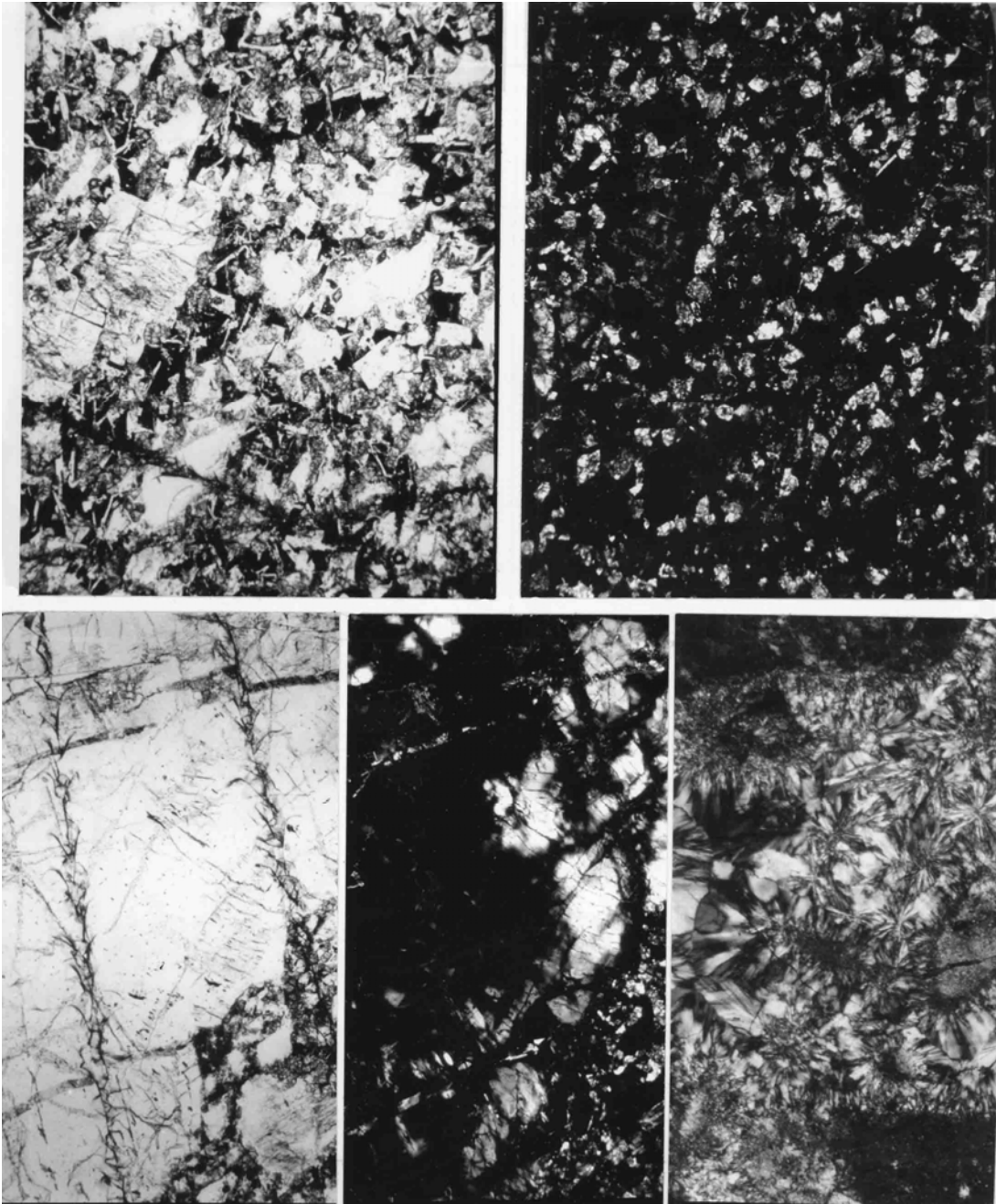


FIGURE 3.

- a) 61016,217. Basaltic area, ppl. Width 2 mm.
- b) 61016,217. Basaltic area, xpl. Width 2 mm.
- c) 61016,217. Shock-melted anorthositic glass, ppl. Width 1.5 mm.
- d) 61016,217. Shock-melted anorthositic glass, xpl. Width 1.5 mm.
- e) 61016,221. Shocked anorthosite, xpl. Width 1.5 mm.

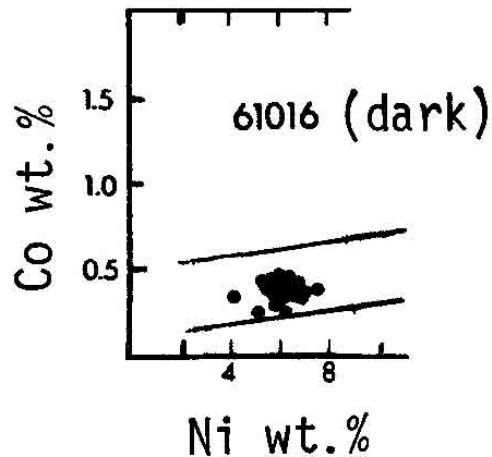


FIGURE 4. Metals, from Misra and Taylor (1975).

The anorthosite is almost pure plagioclase (Table 4) and is at least in part pristine (Krahenbuhl et al., 1973); some analyses have slightly higher siderophile contents and may be contaminated. This would not be surprising in view of the shock-melting, if some of the analyzed samples include shocked glass. (The Ir content of 1620 ppb given by Hughes et al. (1973) is completely anomalous; because it is 3 times higher than chondrites whereas the corresponding Au, Re contents are 5×10^{-4} times chondrites, it is probably erroneous). This pristine chemistry probably does not include volatiles, several of which (e.g., Tl, Cd) are enriched as compared with other ferroan anorthosites.

The glass coat (Table 4) has been analyzed only by the microprobe (Stoffler et al., 1975), thus no trace element data exist. Its major element composition distinguishes it from both local soil and the 61016 basaltic impact melt. It is similar to Station 11 soil.

TABLE 1. Minor Elements in 61016 Anorthosite Plagioclases (Hansen et al., 1979a).

Sample	Mol % Ab	FeO wt%	MgO wt%	K ₂ O wt%
,15	3.5	0.11	0.07	0.006
,27 melted	3.8	0.231	0.17	0.022
,27 non-melted	3.8	0.121	0.051	0.023

STABLE ISOTOPES: Stable isotope data are only available for the basaltic impact melt. These data serve to emphasize that the melt is not melted soil. Rees and Thode (1974) report S isotope data (erroneously referred to as for the anorthosite) showing that $\delta^{34}\text{S}$ is -0.1 ‰ , much lower than soils ($\sim +8 \text{ ‰}$). Kerridge et al. (1975b) confirm the low

value for $\delta^{34}\text{S}$ (+1.9, +1.3 ‰). These latter authors also report $\delta^{13}\text{C}$ results of -35.7, -32.8 ‰ (soils +10‰ or higher). DesMarais (1978) reports $\delta^{34}\text{C}$ of -30.8‰. Allen et al. (1974) report total ^{204}Pb (considered stable because of its extremely long half-life) in the impact melt, and consider that non-leachable ^{204}Pb is partitioned into fine metallic grains.

GEOCHRONOLOGY AND RADIOGENIC ISOTOPES: No Rb-Sr or Sm-Nd internal isochrons exist for any lithologies in 61016, but whole-rock Rb-Sr data are available for both the basaltic impact melt (Table 5) and the anorthosite (Table 6). The anorthosite clearly was separated from high-Rb reservoirs very early in lunar history.

TABLE 2. Chemical work on 61016 basaltic impact melt.

<u>REFERENCE</u>	<u>SPLIT ANALYZED</u>	<u>ELEMENTS ANALYZED</u>
S.R. Taylor <u>et al.</u> (1973)	,149	major and traces
Duncan <u>et al.</u> (1973)	,139	major and traces
Janghorbani <u>et al.</u> (1973)	,133	majors
Rose <u>et al.</u> (1973)	,150	major and traces
Brunfelt <u>et al.</u> (1973)	,145	majors and traces
Hubbard <u>et al.</u> (1973)	,143	majors and traces
Nyquist <u>et al.</u> (1973)		Rb, Sr
Laul and Schmitt (1973)	,152	major, traces, siderophiles
Nakamura <u>et al.</u> (1973)	,148	majors and traces
Wänke <u>et al.</u> (1973)	,151	majors, traces, siderophiles
Wänke <u>et al.</u> (1974)	,151	majors, traces, siderophiles
Wänke <u>et al.</u> (1977)	,151	V
Juan <u>et al.</u> (1974)	,146	majors and traces
Stettler <u>et al.</u> (1973)	,4	K, Ca
Jovanovic and Reed (1973)	,131*	F, Cl, Br, I, Li, U, Te
Allen <u>et al.</u> (1974, 1975)	,131*	^{204}Pb , Bi, Tl, Zn
Jovanovic and Reed (1976a)	,131	Ru, Os
Reed <u>et al.</u> (1977)	,131	Zn, Tl
Eldridge <u>et al.</u> (1973)	,120	K, U, Th
Ehmann and Chyi (1974)	,133	Zr, Hf
Miller <u>et al.</u> (1974)	,133	
Garg and Ehmann (1976)	,133	Zr, Hf, Fe, Co, Sc, Cr, REEs, Th
Des Marais (1978)	,323	N, S, C
Kerridge <u>et al.</u> (1975)	,159, 160	C, S
Goels <u>et al.</u> (1975)	,136	N
Gibson and Moore (1975)		Volatile gas compounds
Rees and Thode (1974)	,137*	S
Krähenbühl <u>et al.</u> (1973)	,132	Meteoritic siderophiles and volatiles
Ganapathy <u>et al.</u> (1974)		

* Erroneously referred to in paper as the anorthosite phase.

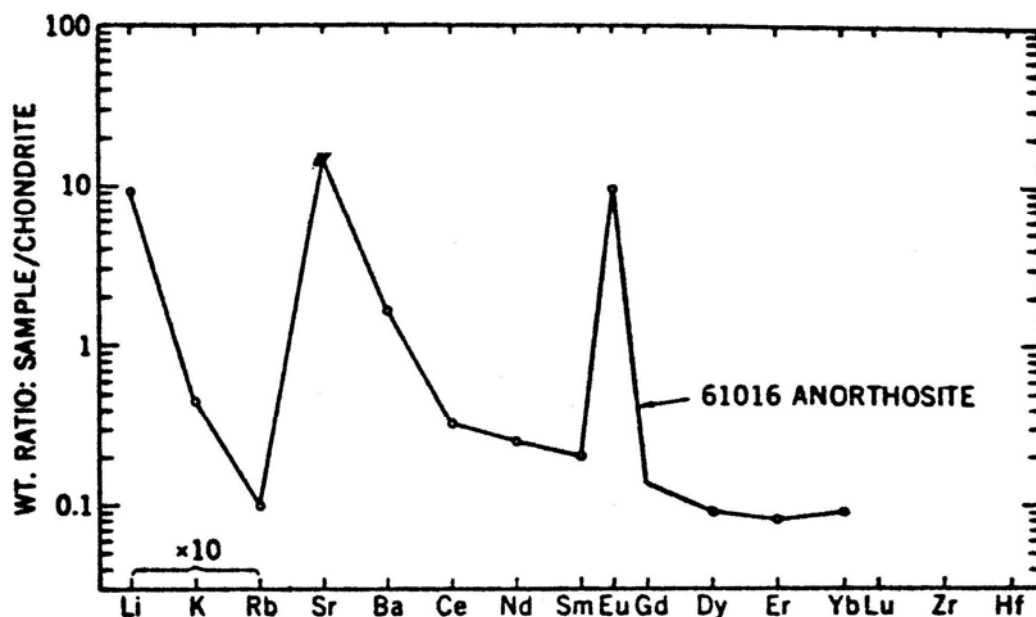


FIGURE 5. Incompatible elements, from Philpotts et al.

TABLE 3. Chemical work on 61016 anorthosite.

<u>REFERENCE</u>	<u>SPLIT ANALYZED</u>	<u>ELEMENTS ANALYZED</u>
Nava (1974)	,184	Majors
Philpotts <u>et al.</u> (1973)	,184	REEs, Ba
Wrigley (1973)	,173	K, U, Th
Fruchter <u>et al.</u> (1974)	,180	Fe, Al, Co, Sc, Cr, REEs
Hubbard <u>et al.</u> (1974)	,79 ,84	Mg, REEs, other traces
Ganapathy <u>et al.</u> (1974)	,156	Siderophiles, volatiles
Wasson <u>et al.</u> (1975)	,161*	Siderophiles, volatiles
Baedecker <u>et al.</u> (1974b)		
Hughes <u>et al.</u> (1973)	,182	Ni, Ir, Au, Re
Tera <u>et al.</u> (1973)	,84	K, Rb, Sr
Nyquist <u>et al.</u> (1973)	,79 ,84	Rb, Sr
LSPET (1973)	,3**	Majors, traces

* ,161 in data pack is a dark chip. White chip intended for allocation to Wasson was ,183; the numbers evidently have become reversed.

** Mixed powder, severely contaminated with basaltic impact melt.

TABLE 4. Summary chemistry of lithologies in 61016.

	<u>Basaltic Impact Melt</u>	<u>Anorthosite</u>	<u>Glass Coat</u>
SiO ₂	43.3	45.0	44.5
TiO ₂	0.76	0.02	0.17
Al ₂ O ₃	25.1	34.6	29.8
Cr ₂ O ₃	0.10	0.01	
FeO	5.1	0.3	3.7
MnO	0.05	<0.01	
MgO	10.7	0.2	4.9
CaO	14.3	19.6	15.6
Na ₂ O	0.33	0.40	0.66
K ₂ O	0.08	0.01	0.08
P ₂ O ₅	0.12	0.05	0.08
Sr	160	180	
La	15.3	0.1	
Lu	0.65	0.01	
Rb	2.0	0.1	
Sc	6.6	0.5	
Ni	443	~1.0	
Co	36	~1.0	
Ir ppb	13	0.01 ?	
Au ppb	12	0.02	
C	35	--	
N	19	--	
S	538	100	
Zn	~1	1.6	
Cu	4.4	--	

Oxides in wt%; others in ppm except as noted.

⁴⁰Ar-³⁹Ar data are available for the basaltic impact melt (Stettler et al., 1973) and the shocked anorthosite (Huneke et al., 1977). A dark split, 4 gave an age of 3.65 ± 0.04 b.y. (Fig. 6) but a good plateau was not attained (Stettler et al., 1973). Huneke et al. (1977) analyzed both clear and milky "diaplectic glasses" (Fig. 7). The age spectra are anomalous, and the clear glass is shifted to Younger ages, with an apparent age for the milky glass clearly defined at 4.1 b.y. Huneke et al. (1977) suggest that shock melting can result in glass with distinctly different age plateaus. Neither glass records the true age of the anorthosite.

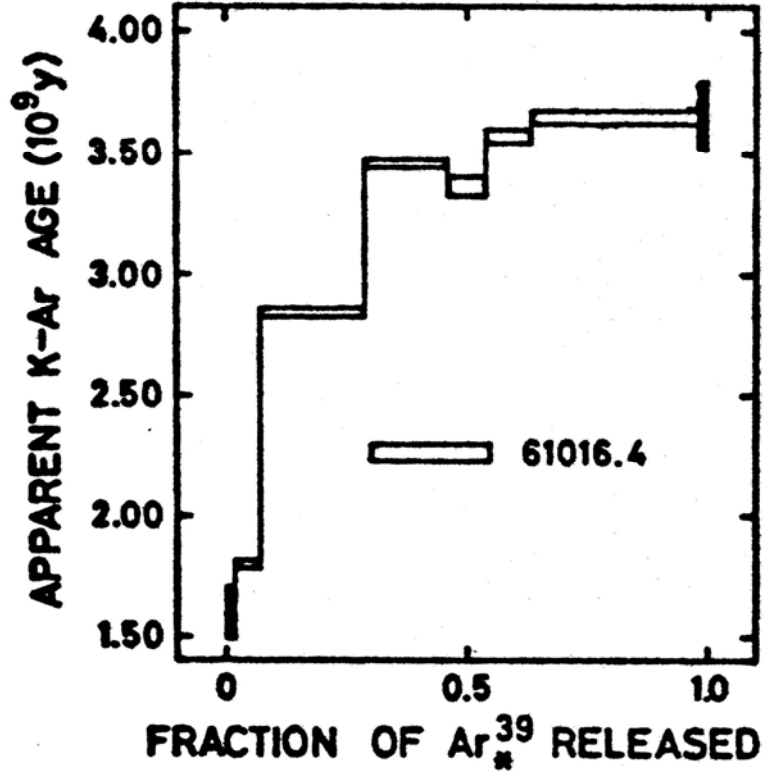


FIGURE 6. Ar releases of basaltic melt, from anorthositic glasses, from Stettler et al. (1973).

TABLE 5. Rb-Sr isotopic data for 61016 basaltic impact melt (from Nyquist et al., 1973)

Sample	Rb ppm	Sr ppm	$^{87}\text{Sr}/^{86}\text{Sr}$	T_{BABI} (b.y.)
,143 crystalline	2.04	164.4	0.70139±8	4.50±0.16
,79 black glassy	1.877	145.4	0.70151±10	4.49±0.33
,3 powder: mixed anorthosite & basalt	0.446	177.9	0.69960±9	4.8±0.1

RARE GAS EXPOSURE AGES AND SURFACES: Stettler et al. (1973) calculate a ^{37}Ar - ^{38}Ar exposure age of <7 m.y. from a dark surface chip. This age is probably affected by ^{37}Cl because the Cl content of the rock is high and the exposure age is low. ^{38}Ar is produced from ^{37}Cl during pile irradiation and this effect is probably responsible for the unusual release curve observed (Stettler et al., 1973).

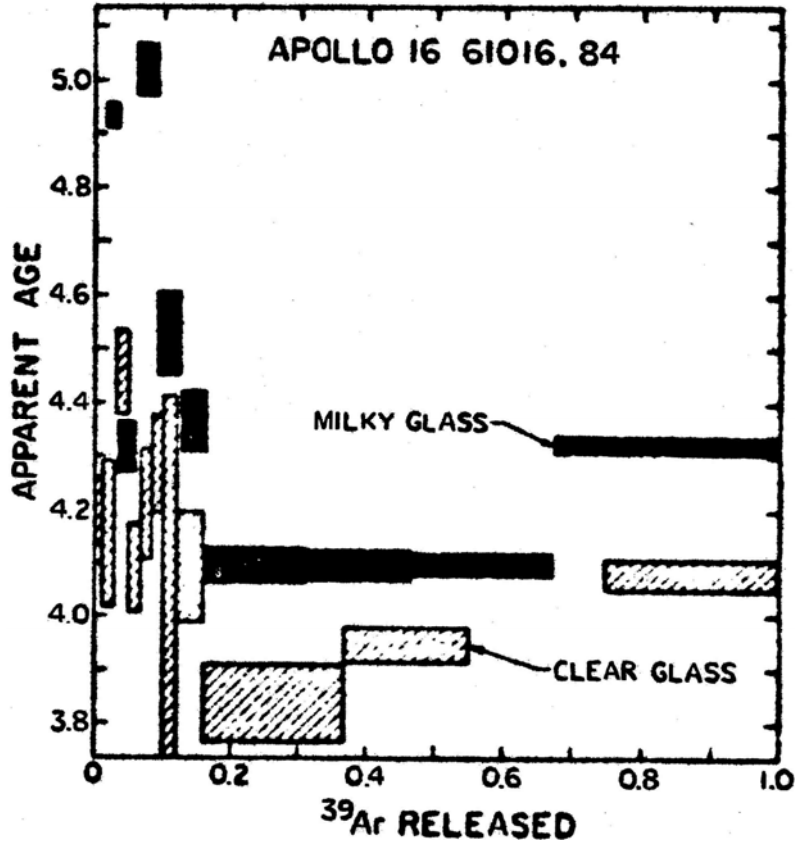


FIGURE 7. Ar releases of anorthositic glasses, from Huneke et al. (1977).

TABLE 6. Rb-Sr isotopic data for 61016 anorthosite.

Sample	Rb ppm	Sr ppm	$^{87}\text{Sr}/^{86}\text{Sr}$	$^{87}\text{Sr}/^{86}\text{Sr}^*$ calc. at 4.6 b.y.	Reference
,79 gray gray, repeat	0.017 ^a	179.0	0.69906±5 ^b 0.69906±5 ^b	0.69892±5 0.69892±5	Nyquist <i>et al.</i> (1793)
,79 white white, repeat white, repeat	0.0377	180.4	0.69924±40 0.69926±22 0.69906±4 ^{b,c}	- - 0.69890±4	Nyquist <i>et al.</i> (1973)
,79	0.0250	184.7	0.69907±3	0.69892±3	Nyquist <i>et al.</i> (1979)
,84	0.040	181.7	0.69907±5 ^b	0.69891±5	Nyquist <i>et al.</i> (1973)
,84	0.032 0.044	178 180	0.69900±3 0.69900±4	0.69897±3 0.69895±4	Tera <i>et al.</i> (1973)

*Corrected for interlaboratory bias to conform with CalTech data where applicable.
a) Misprinted as 0.167 in original paper.
b) Corrected according to Nyquist *et al.* (1974, p. 1519) for error caused by tracer.
c) Preferred value for this sample (Nyquist, pers. comm.).

Rao et al. (1979) use quantitative techniques to isolate the solar cosmic ray-produced Ne and Ar components in three sampling intervals from ,287 (which contains anorthosite and glass surface material). A solar cosmic ray age of 1.7 ± 0.2 m.y. is derived, as well as a galactic cosmic ray age of 3.7 ± 0.3 m.y. An erosion rate of 5 mm/m.y. is assumed.

Fleisher and Hart (1974) studied the particle track record (heavy cosmic ray nuclei). Two dark chips were too heavily shocked to reveal tracks. An anorthosite surface chip has an unusual track density/depth profile suggesting recent loss of a 1 mm chip. Assuming negligible erosion, an exposure age of 20 m.y. is calculated; assuming $0.6 \text{ \AA}/\text{year}$ erosion, an exposure age of 40 m.y. is calculated. This is consistent with ^{26}Al data (Eldridge et al., 1973) which is saturated in the surface indicating exposure of more than a few million years. Bhattacharya and Bhandari (1975), evaluating erosional effects on the track record, derive an exposure age of 1.5 m.y. for the surface chip ,287. Bhandari et al. (1975) calculate an age of 1.2 ± 0.4 m.y. based on large craters, and 0.5 m.y. based on craters less than $80 \text{ }\mu\text{m}$ in diameter. They suggest a simple one-stage exposure history. Bhandari et al. (1975, 1976) also measured ^{26}Al with depth and conclude that there has been little variation in the average solar flare proton production over the last 1.5 m.y.

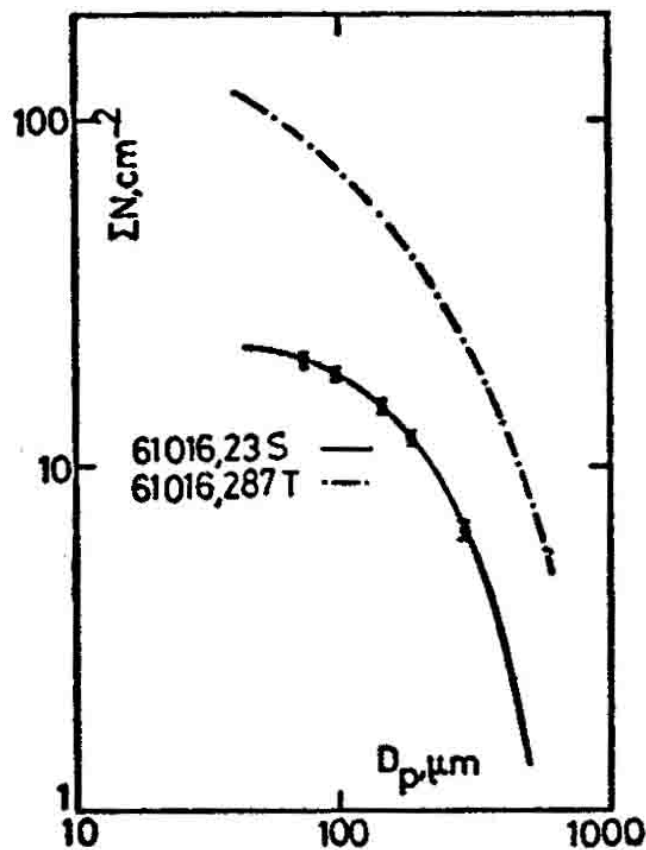


FIGURE 8. Microcraters, from Mandeville et al. (1976).

MacDougall et al. (1973) found no solar flare tracks in either olivine or feldspar in an anorthosite sample.

Mandeville (1976) studied the size distribution of microcraters on a chip of impact melt (,23). The sample has fewer craters than the sample studied by Bhandari et al. (1975) which was on the lunar top of the sample (Fig. 8). Depth/pit diameters are also reported.

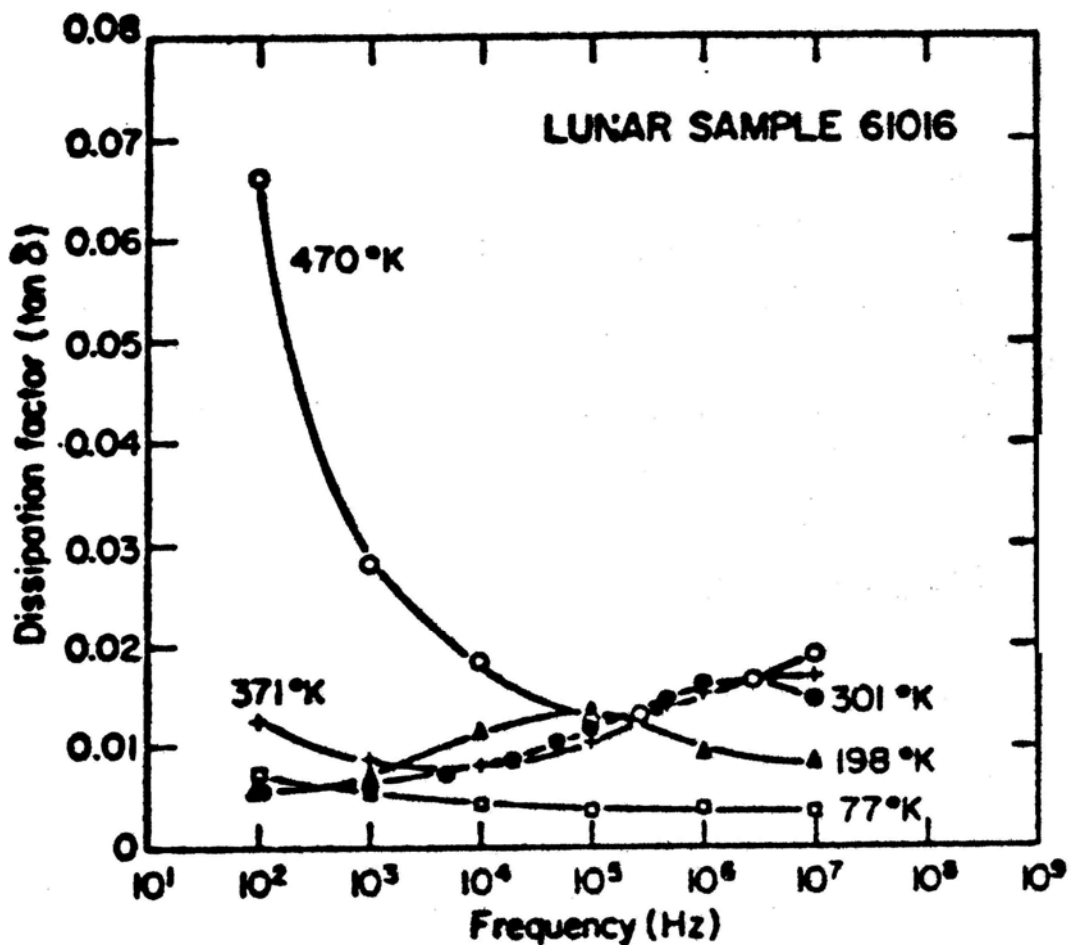
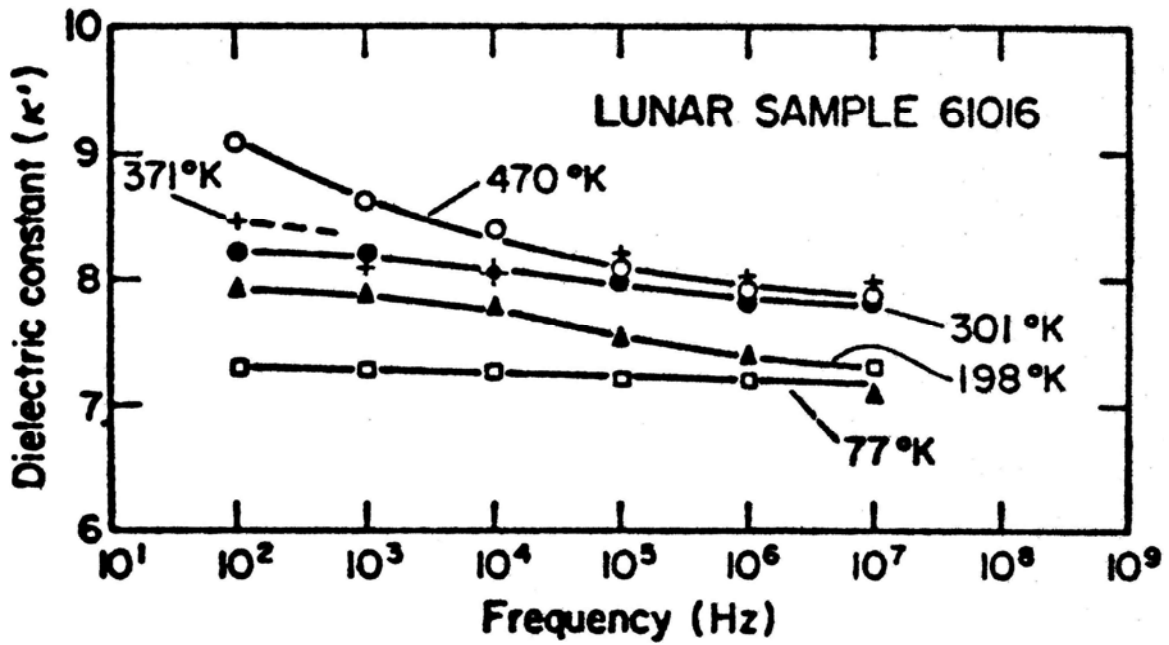
Gold et al. (1976a) report auger spectrometer analyses for Fe, Ti, Ca and Si (normalized to 60017 values) for a chip of basaltic impact melt. Fe is enriched in the surface.

PHYSICAL PROPERTIES: Stephenson et al. (1977) tabulate, without comment, magnetic data for a glass chip from 61016. Housley et al. (1976) found that the ferromagnetic remanence (FMR) of a chip of basaltic impact melt (,27) was extremely weak.

Chung and Westphal (1973) provide dielectric constant, dielectric losses, and electrical conductivity data as a function of frequency and temperature. These data (Fig. 9) are for a chip of basaltic impact melt. The seismic data of Chung (1973) are for the same chip. Elastic wave (P-and S-) velocities were measured as a function of pressure as received and in both “dry” and “wet” modes (Table 7, Fig. 10). At low pressures, water increases velocities and drying the sample decreases velocities; this effect is greatest for P-waves. Warren and Trice (1975) use Chung’s (1973) data to plot dynamic compressional modulus/density against pressure. They erroneously refer to the data as being for the anorthosite.

Dollfus and Geake (1975) report polarimetric and photometric characteristics of light reflected from a sample of dust-covered, surface basaltic impact melt (,23). The polarization curves resemble lunar fines.

PROCESSING AND SUBDIVISIONS: 61016 has been extensively subdivided. In 1972 a slab was cut from the rock producing two end pieces ,7 and ,8 (Figs. 1 and 11). ,7 remains essentially intact. The slab has been extensively dissected (Figs. 2 and 11) and ,8 has been totally subdivided into numerous daughters (not shown).



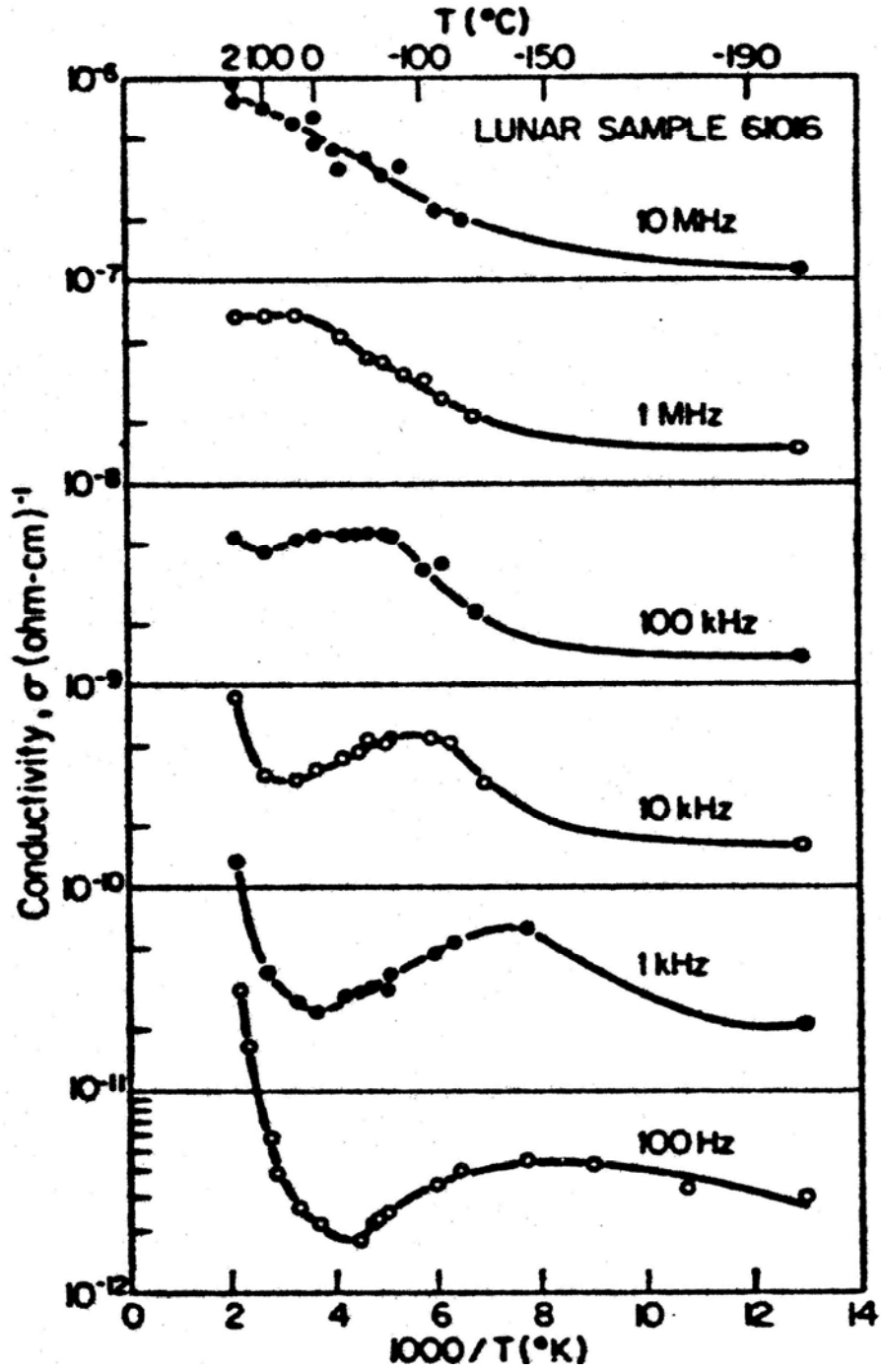


FIGURE 9. Electrical data, from Chung and Westphal (1973).

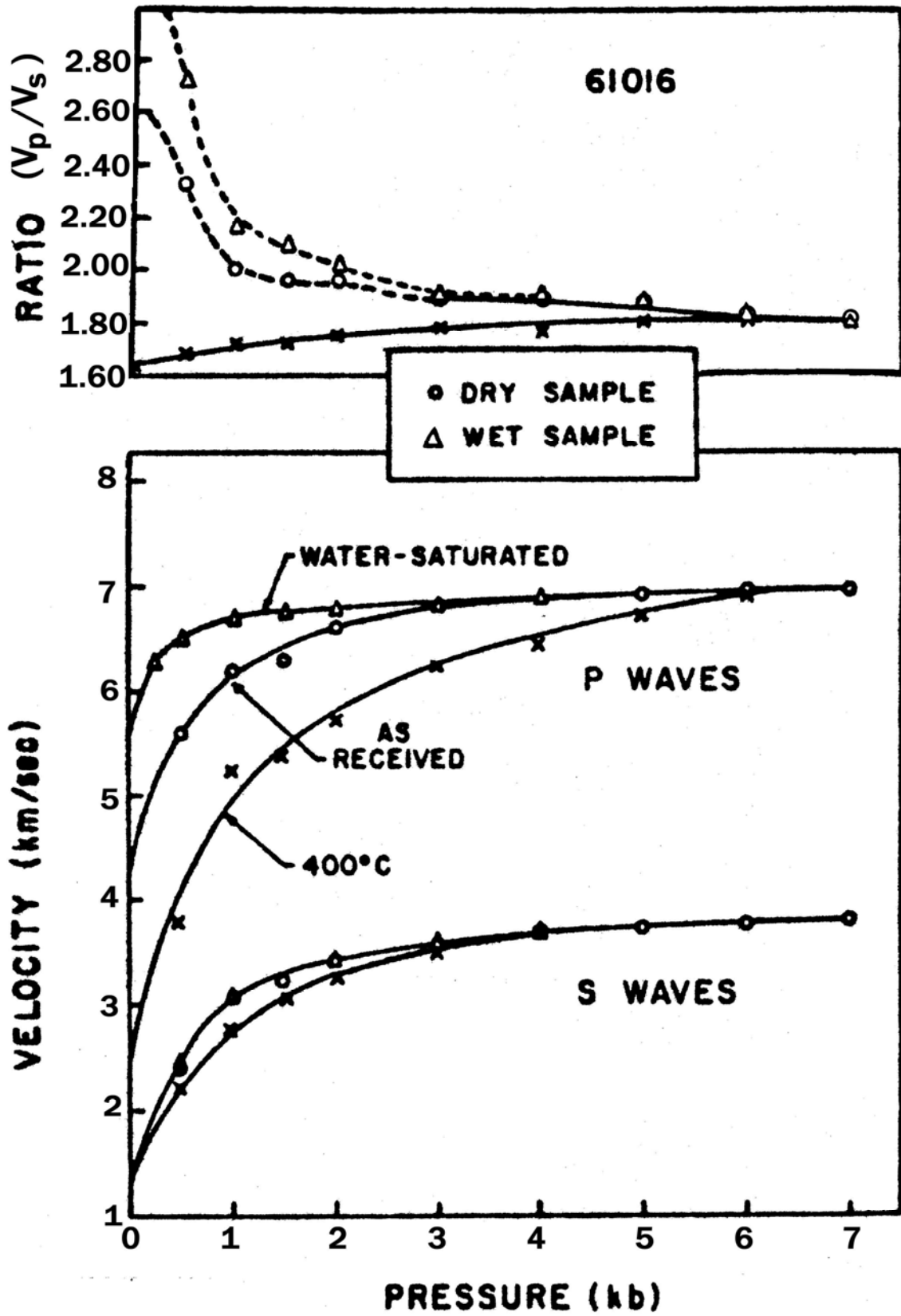


FIGURE 10. Seismic data, from Chung (1973).

TABLE 7. Seismic data, from Chung (1973).

Condition of Sample	Mode	0.5	1.0	1.5	2	3	4	5	6	7	(10)*
As Received (from Table 2)	P	5.6	6.2	6.30	6.60	6.77	6.87	6.91	6.96	6.99	7.02
	S	2.4	3.1	3.22	3.36	3.58	3.69	3.74	3.86	3.88	3.90
	V_p/V_s	2.3	2.0	1.96	1.96	1.89	1.86	1.84	1.80	1.80	1.80
"dry" (1)	P	3.75	5.23	5.32	5.72	6.23	6.41	6.70	6.97	7.00	7.02
	S	2.23	3.04	3.09	3.25	3.52	3.64	3.72	3.86	3.88	3.90
	V_p/V_s	1.68	1.72	1.72	1.76	1.77	1.76	1.80	1.80	1.80	1.80
"wet" (2)	P	6.5	6.70	6.73	6.75	6.78	6.88	6.91	6.97	6.99	7.03
	S	2.4	3.10	3.23	3.36	3.58	3.69	3.74	3.86	3.88	3.90
	V_p/V_s	2.7	2.16	2.09	2.01	1.89	1.86	1.84	1.80	1.80	1.80

*Estimated by a linear extrapolation of high-pressure velocity data.
 (1) The term "dry" refers to the state of sample 61016 as it was heated in vacuum at 400°C for 10 hours and slowly cooled down to ambient temperature.
 (2) The term "wet" refers to a water-saturated sample 61016.

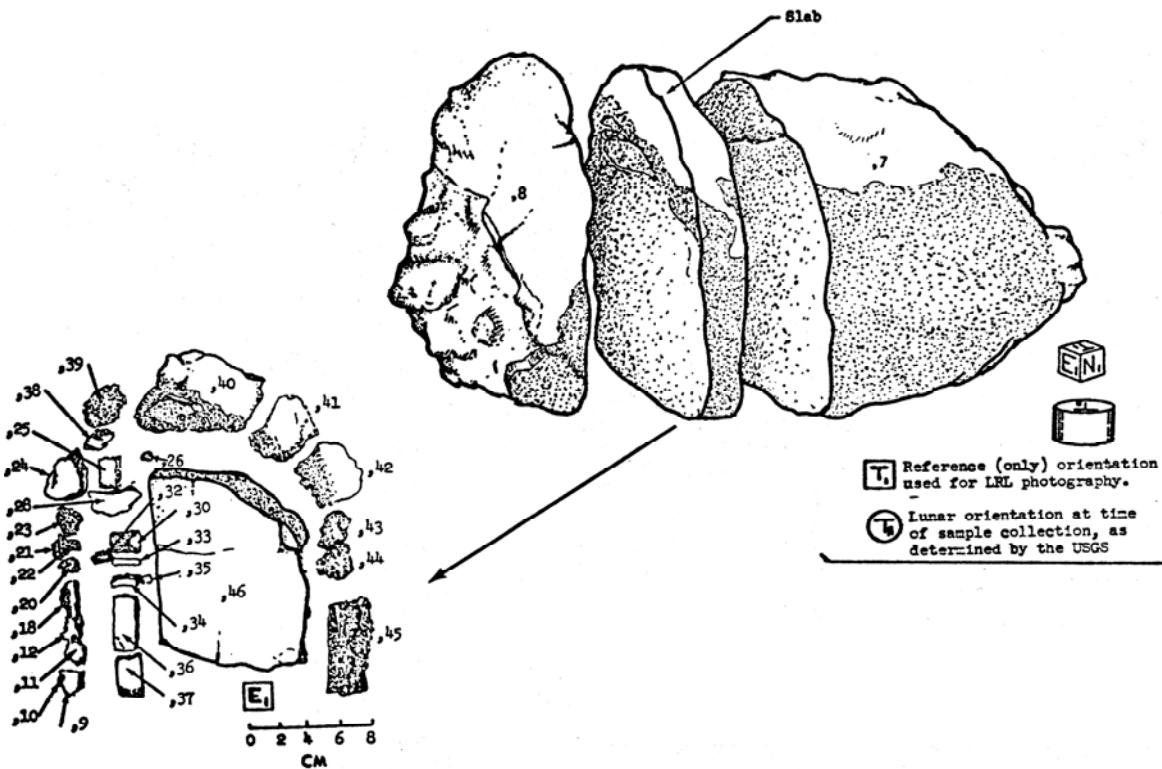


FIGURE 11. Cutting diagram.